Single-Molecule Structural Dynamics of EF-G−Ribosome Interaction during Translocation†

Yuhong Wang,‡ Haiou Qin,§ Rama D. Kudaravalli,‡ Stanislas V. Kirillov,§,|| Graham T. Dempsey,‡ Dongli Pan,§ Barry S. Cooperman,*,§ and Yale E. Goldman*,‡

Pennsylvania Muscle Institute, School of Medicine, University of Pennsylvania, Philadelphia, Pennsylvania 19104-6083, and Department of Chemistry, University of Pennsylvania, Philadelphia, Pennsylvania 19104-6323

Received April 6, 2007; Revised Manuscript Received July 13, 2007

ABSTRACT: EF-G catalyzes translocation of mRNA and tRNAs within the ribosome during protein synthesis. Detection of structural states in the reaction sequence that are not highly populated can be facilitated by studying the process one molecule at a time. Here we present single-molecule studies of translocation showing that, for ribosomes engaged in poly(Phe) synthesis, fluorescence resonance energy transfer (FRET) between the G′ domain of EF-G and the N-terminal domain of ribosomal protein L11 occurs within two rapidly interconverting states, having FRET efficiencies of 0.3 and 0.6. The antibiotic fusidic acid increases the population of the 0.6 state, indicating that it traps the ribosome•EF-G complex in a preexisting conformation formed during translation. Only the 0.3 state is observed when poly(Phe) synthesis is prevented by omission of EF-Tu, or in studies on vacant ribosomes. These results suggest that the 0.6 state results from the conformational lability of unlocked ribosomes formed during translocation. An idling state, possibly pertinent to regulation of protein synthesis, is detected in some ribosomes in the poly(Phe) system.

Protein synthesis by mRNA-programmed bacterial ribosomes proceeds in four distinct phases: initiation, peptide elongation, termination, and recycling. Each cycle of the elongation phase is a multistep process, including binding of aminoacyl-tRNA (aa-tRNA)[1] as a ternary complex with elongation factor EF-Tu and GTP, accommodation of aa-tRNA into the A-site of a ribosome containing peptidyl-tRNA in the P-site, transfer of the peptidyl moiety to the aa-tRNA, lengthening the nascent peptide chain by one amino acid and forming the pretranslocation complex, and, finally, translocation of the two tRNAs into the P-site and exit site (E-site), with corresponding movement of the two cognate mRNA triplet codons. Translocation is catalyzed by elongation factor EF-G, complexed with GTP. X-ray and cryo-EM structural studies (*1*−*8*) have revolutionized our understanding of elongation at the molecular and atomic level, showing, for example, that factors EF-Tu and EF-G bind to a common location within the ribosome, but to different intermediate states of the elongation cycle (*9*). However, the dynamics that connect the intermediates in the elongation phase are not known in sufficient detail to fully understand its mechanism.

Formation of the pretranslocation complex places discharged tRNA at the P-site and results in a conformationally labile ribosome structure that undergoes a ratchetlike rotation of the 30S subunit relative to the 50S subunit on EF-G−GTP binding and GTP hydrolysis (*10*, *11*). This rotation is accompanied by movements of the L1 stalk and motion of the G′ domain of EF-G toward the N-terminal domain (NTD) of L11, a component of the GTPase activation center (GAC) (*12*−*15*). These large-scale conformational changes are rapidly propagated to the tRNA binding sites (*11*, *16*), facilitating the tRNA movements that are required for translocation. Exactly how the energy liberated by GTP hydrolysis induces the conformational changes within the ribosome•EF-G complex, leading to translocation, remains unclear, although the hydrolysis step is known to be important both catalytically and thermodynamically (*16*, *17*).

Single-molecule studies have the potential to help elucidate the reaction sequence of translocation by identifying mechanistically important intermediates that may be too short-lived and/or weakly populated to be detected by conventional ensemble kinetic measurements. Recent single-molecule studies have demonstrated the utility of this approach for elucidating the process of codon recognition on the ribosome (*18*−*20*). Here we report single-molecule fluorescence resonance energy transfer (smFRET) experiments that focus on the motions of the G′ domain relative to L11-NTD during EF-G-catalyzed translocation in an elongation system employing poly(U) programmed ribosomes to synthesize polyphenylalanine [poly(Phe)]. The ribosomes were immobilized on a glass surface for smFRET measurements by total internal reflection microscopy (TIRF). The experiments reveal a new

† This work was supported by NIH Grants GM63205 and GM71014 and NSF Grant NSEC DMR-0425780. Y.W. is an NIH Ruth L. Kirschstein Postdoctoral Fellow.

* To whom correspondence should be addressed. Y.E.G.: phone, (215) 898-4017; fax, (215) 898-2653; e-mail, goldmany@mail.med.upenn.edu. B.S.C.: phone, (215) 898-6330; e-mail, cooprman@pobox.upenn.edu.

‡ Pennsylvania Muscle Institute, School of Medicine.

§ Department of Chemistry.

|| Current address: Petersburg Nuclear Physics Institute, Russian Academy of Science, 188300 Gatchina, Russia.

[1] Abbreviations: smFRET, single-molecule fluorescence resonance energy transfer; TIRF, total internal reflection microscopy; aa-tRNA, aminoacyl-tRNA; NTD, N-terminal domain; GAC, GTPase activation center; poly(Phe), polyphenylalanine.

10.1021/bi700657d CCC: $37.00
Published on Web 08/30/2007

intermediate state that exhibits a FRET efficiency higher than that previously seen in ensemble experiments (*15*), and they elucidate the mechanism of inhibition of elongation by the antibiotic fusidic acid. A nontranslocating idling state that may play a role in regulating ribosome activity in the cell was identified. The results have been briefly reported in abstract form (*21*).

MATERIALS AND METHODS

Buffers. Solutions were prepared and adjusted to their final pH at 25 °C. TAM_{10} buffer: 20 mM Tris (pH 7.5), 30 mM NH_4Cl, 70 mM KCl, 10 mM $MgAc_2$, and 1 mM DTT. MonoS FPLC column gradient buffer for L11 purification: 20 mM Tris (pH 7.1), 1 mM EDTA, 6 M urea, and 100−800 mM NH_4Cl. L11 storage buffer: 20 mM Hepes (pH 7.6), 400 mM NH_4Cl, 20 mM $MgCl_2$, 1 mM EDTA, and 4 mM β-mercaptoethanol (BME). L11 labeling buffer: 50 mM Tris (pH 7.5) and 400 mM NH_4Cl. AM77 storage buffer: 20 mM Hepes (pH 7.6), 30 mM NH_4Cl, and 6 mM $MgCl_2$. W buffer: 50 mM Tris (pH 7.6), 30 mM NH_4Cl, 70 mM KCl, 7 mM $MgCl_2$, and 1 mM DTT. Cy5-labeled 50S storage buffer: 20 mM Tris (pH 7.5), 15 mM $MgAc_2$, 30 mM NH_4Cl, 70 mM KCl, 0.5 mM EDTA, and 7 mM BME. 70S mixing buffer: 20 mM Tris (pH 7.5), 10 mM $MgCl_2$, 100 mM NH_4Cl, and 1 mM BME. EF-G labeling buffer: 50 mM Hepes (pH 7.5), 100 mM NaCl, and 1 mM $MgCl_2$. EF-G storage buffer: 50 mM Tris (pH 8.0), 200 mM NaCl, 20% glycerol, and 1 mM DTT.

Ribosomes Lacking L11, Cy5-L11, and Labeled Ribosomes. Mutant ribosomes lacking L11 were isolated from *Escherichia coli* strain AM77 as described previously (*22*) except that tightly coupled ribosomes were purified by ultracentrifugation in buffer containing 8 mM Mg^{2+}. 50S and 30S subunits were prepared from these tightly coupled ribosomes by zonal centrifugation in a buffer containing 2 mM Mg^{2+} and 200 mM NH_4Cl. His-tagged L11 was purified as described previously (*15*) except that, following chromatography on a Ni-NTA column (Qiagen), an additional chromatographic step on a MonoS FPLC column was employed to remove a contaminating protein with a higher molecular weight. For labeling with Cy5, L11 was concentrated (Centricon YM-10), exchanged into L11 labeling buffer using a Nap-5 column (Amersham Biosciences, 0.9 cm × 2.8 cm), and adjusted to 1 mg/mL. Fifty microliters of ~10 mM Cy5-maleimide (Amersham Biosciences) in DMF was added dropwise with stirring to 1 mL of protein solution and the mixture incubated for 1 h at 37 °C. The reaction was quenched with 3 μL of 14 M BME. Unreacted Cy5 was removed by a combination of Sephadex G-25 gel chromatography (1 cm × 35 cm) and Centricon YM-10 filtration. The Cy5:protein ratio was 0.9, measured by Cy5 absorbance (ϵ_{652} = 250 000 M^{-1} cm^{-1}) and the Bradford assay (0.6 μg of L11 yields the same color increase as 1.0 μg of bovine serum albumin). AM77 50S subunits were biotinylated as follows: 400 A_{260} units in TAM_{10} (300 μL) was exchanged into 100 mM sodium acetate (NaAc, pH 7.0) using a Nap-5 column. The resulting 1 mL of 50S subunit in NaAc was oxidized by $NaIO_4$ (2 mM) on ice for 10 min in the dark. The reaction was then quenched by incubation with 5 mM Na_2SO_3 and 10 mM $MgAc_2$ for 10 min. Biotinylation was carried out with 5 mM biotin-XX hydrazide [6-((6-((biotinoyl)amino)hexanoyl)amino)hexanoic acid, hydrazide, Molecular Probes, B-2600] with gentle stirring for 2 h at room temperature. The volume of the final reaction solution was reduced to ≤300 μL by centrifugation (Centricon YM-10), and unreacted biotin-XX hydrazide was removed by chromatography on a Sephadex G25 column (1 cm × 25 cm).

The percentage of biotinylation of the 50S subunits was estimated by a bead binding assay, in which 50S subunits (0.5 A_{260} unit) in TAM_{10} buffer (200 μL) were shaken gently with 0.5 mg of streptavidin-coated magnetic beads (1 μm diameter, Roche) for 15 min. The beads were then separated from the ribosome loading buffer and washed twice with TAM_{10} buffer. The percentage of ribosomal subunits bound to the beads, typically 70%, was determined from the difference in A_{260} units in the original solution and in the sum of the first supernatant and two washes.

Cy5-labeled 50S subunits were formed by incubating biotinylated AM77 50S (1 nmol) with a slight excess of Cy5-L11 (as measured by the 652 nm Cy5 absorbance) in 1 mL of W buffer for 15 min at 37 °C. Excess dye was removed by centrifugation (56 600 rpm; Ti 70.1 rotor; 18 h) through a sucrose cushion (1.1 M sucrose in W buffer), yielding a 50S pellet which was taken up in Cy5-labeled 50S storage buffer. The Cy5:50S ratio was 0.9 ± 0.1. Cy5-labeled 70S ribosomes were obtained by mixing Cy5-labeled 50S subunits with a 1.5-fold excess of 30S subunits in 70S mixing buffer.

EF-G Mutants and Labeling. A cysteine-free mutant of *E. coli* EF-G in vector pET24b was obtained from K. S. Wilson (University of Alberta, Edmonton, AB). Glu^{231} was mutated to Cys using the QuikChange site-directed mutagenesis kit (Stratagene). The EF-G E231C mutant protein was overexpressed in *E. coli* BL21 pLysS cells and purified on a Ni-NTA column (Qiagen) with EF-G storage buffer.

For labeling with Cy3 at the single native Cys residue at position 38, TCEP [1,2,3-tris(2-cyanoethoxy)propane, Sigma], 50 μM, was added to the EF-G mutant protein (50 μM) in the labeling buffer and the solution was incubated at room temperature for 40 min. A 5-fold excess of the Cy3-maleimide (Amersham Biosciences) was added, and the reaction mixture was incubated for 2 h at room temperature in the dark. After the reaction had been quenched with BME, the reaction mixture was passed through a Nap-10 column (Amersham Biosciences) to remove unreacted dye. The labeled protein was further purified, and unlabeled protein was removed via FPLC using a TSK phenyl-Sepharose column (Tosoh Bioscience, 5PW) with a gradient from high-salt buffer [20 mM Hepes (pH 7.0) and 3.5 M NaCl] to low-salt buffer [20 mM Hepes (pH 7.0) and 100 mM NaCl]. The labeled protein was stored at −80 °C in EF-G storage buffer. The dye:protein ratio was 1:1 in the final purified solution. The labeled EF-G is fully active compared to the wild type (Supporting Information, Figure S1).

Other Reagents. Plasmids for expression of EF-Tu, with a C-terminal His tag, were a gift from M. Sassanfar (Harvard University, Cambridge, MA), and EF-Ts with an intein chitin-binding domain at the C-terminus was a gift from H. Karring (Aarhus University, Aarhus, Denmark). The EF-Tu

protein was purified on Ni-NTA columns. The EF-Ts protein was purified on chitin columns from New England Biolabs, Inc. $tRNA^{Phe}$ was purchased from Chemblock. *N*-Acetylphenylalanine-tRNA was prepared essentially as described previously (*23*). Purified $tRNA^{phe}$ aminoacyl synthetase was a gift from Y. Hou (Thomas Jefferson University, Philadelphia, PA). All the other reagents were purchased from Sigma-Aldrich.

Poly(Phe) Assay. In a typical poly(Phe) assay, three mixtures were made: (1) the ribosome mixture containing 1 μM ribosomes, 1 mg/mL poly(U) (Sigma), and 1 μM *N*-acetylphenylalanine-tRNA in TAM_{10} buffer; (2) the factor mixture containing 4 μM EF-Tu, 6 μM EF-Ts, 2 μM EF-G, 0.5 mM GTP, 0.5 mM PEP, and 0.006 mg/mL pyruvate kinase in TAM_{10} buffer; and (3) the aminoacylation mixture containing 100 mM Tris (pH 7.5), 20 mM $MgAc_2$, 1 mM EDTA, 4 mM ATP, 7 mM BME, 33 mg/mL purified $tRNA^{phe}$ aminoacyl synthetase, 50 mM ^{14}C-labeled phenylalanine, and 5 mM tRNA. All three mixtures were incubated separately at 37 °C for 10 min. Then 10 μL of the ribosome mixture, 20 μL of the factor mixture, and 20 μL of the aminoacylation mixture were mixed together gently to form the poly(Phe) assay solution. Ten microliters of the poly(Phe) assay solution was sampled at 10 s, 20 s, 30 s, 1 min, and 2 min and added to 500 μL of cold TCA with 0.6 mM phenylalanine on ice. The TCA solutions were then boiled at 90 °C for 10 min and cooled on ice for at least an additional 10 min before being filtered onto nitrocellulose filters so that precipitated poly(Phe) could be retained. Each filter was washed with 6 mL of cold TCA solution and air-dried. The radioactivity of the synthesized polyphenylalanine on each filter was counted by liquid scintillation.

Ensemble FRET Measurements. Fluorescence emission spectra of ensemble FRET between Cy3-EF-G E231C (donor) and Cy5-L11-C38 ribosomes (acceptor) were recorded using a Photon Technology International Quantamaster Fluorometer at an excitation wavelength of 514 nm. Fluorescence emission spectra were collected with a FRET donor only (the solution contained labeled EF-G and unlabeled ribosomes), an acceptor only, a donor and an acceptor (labeled EF-G and labeled ribosomes), and a donor and an acceptor in the presence of 100 μM fusidic acid. The solutions contained 0.36 μM ribosomes and 0.1 μM EF-G in TAM_{10} buffer in the presence of 1 mM GTP. As the ribosomes (FRET acceptors) were present in excess to ensure the efficient FRET from most of the donors, FRET efficiency values were calculated from the decrease in donor fluorescence intensities rather than from the sensitized acceptor emission.

TIRF Measurements on Immobilized Ribosomes. The setup was built on a modified Olympus IX70 microscope. A 10−20 mW, 514 nm laser beam (Melles Griot) was projected into the sample chamber through a 60 × 1.45 NA oil emersion objective (Olympus) and index-matching liquid at a glancing angle relative to the microscope slide. Total internal reflection generated evanescent waves near the sample chamber surface. Fluorophores bound to the surface (but not those in the bulk medium) were optically excited and emitted fluorescence or transferred their energy to nearby fluorophores via FRET. A spectral wavelength separator, Dual View (Optical Insights Corp., Tucson, AZ), filtered out scattered laser light and projected fluorescent images from the donor and acceptor separately onto two halves of the camera CCD chip.

The sample flow chamber (10 μL) was formed from two glass coverslips (Fisher Scientific), spin-coated with 2 mg/mL PMMA (Aldrich Chemical) in methylene chloride, and held together by double-sided adhesive tape that served as spacers and borders of the flow chamber (*24*). Biotinylated ribosomes were bound to the surface PMMA through biotinylated BSA and streptavidin (*24*). All of the buffers used in the single-molecule experiments contained 0.05% Tween 20 detergent (Aldrich) to minimize nonspecific binding of ribosomes to the surfaces. Solution changes were carried out by passing several sample volumes through the flow chamber and wicking the outflow away with filter paper.

For observations on vacant ribosomes, the flow chamber was filled with 0.25 mM GTP and 10 nM Cy3-EF-G in TAM_{10} buffer. For measurements during elongation [poly(Phe) system], 1 μM ribosomes were preincubated with 1 mg/mL poly(U) mRNA (Sigma) and 1 μM *N*-acetylphenylalanine-tRNA before binding to the surface. The flow chamber was then filled with the following solution: 0.1 mg/mL poly(U), 0.25 mM GTP, 0.25 mM phosphoenolpyruvate, 0.01 mg/mL pyruvate kinase, 20 mM Tris buffer (pH 7.5), 10 mM $MgAc_2$, 0.5 mM EDTA, 2 mM ATP, 1 mM DTT, 0.8 μM $tRNA^{phe}$, 32 μg/mL $tRNA^{phe}$ synthetase, 30 μM phenylalanine, 50 nM EF-Tu/EF-Ts, 10 nM Cy3-EF-G, and 0.05% Tween 20. A deoxygenation enzyme system (*25*) of 3 mg/mL glucose, 100 μg/mL glucose oxidase, and 48 μg/mL catalase was present in the final single-molecule imaging solutions to diminish photobleaching. For the fusidic acid experiments, 100 μM antibiotic was added to the final

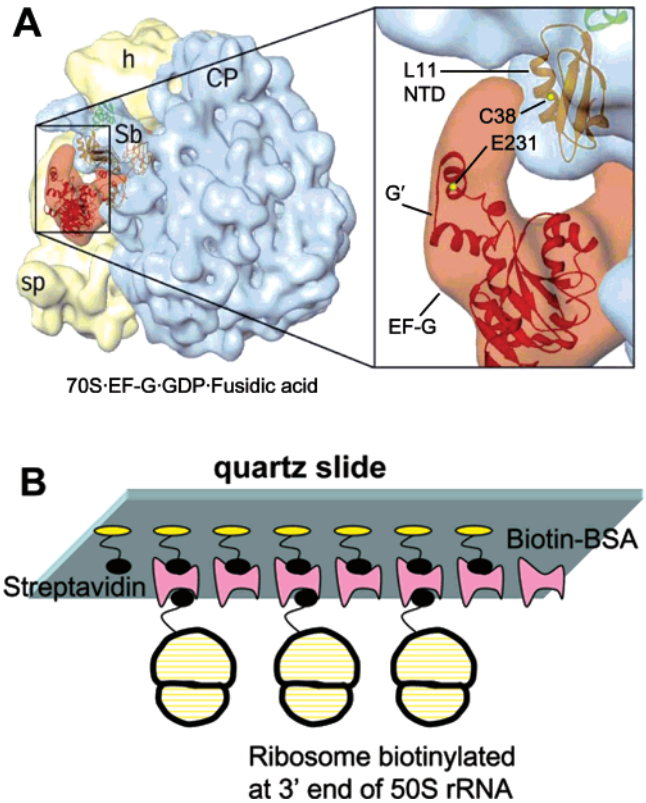

FIGURE 1: (A) Relative positions of Cys^{38} on the N-terminal domain (NTD) of protein L11 and Cys^{231} on EF-G and labeling positions in the ribosome·EF-G complex, adapted from ref *13*. (B) Schematic illustration of the linkage for immobilizing ribosomes onto a surface.

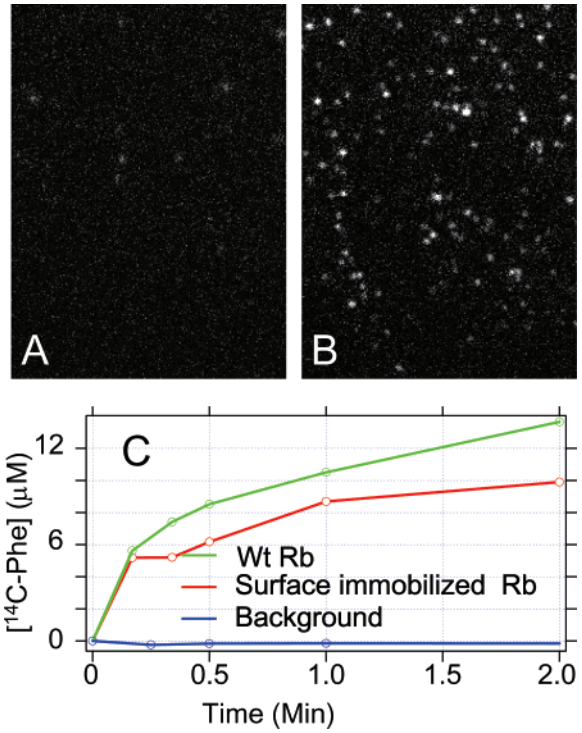

FIGURE 2: Specific binding of biotinylated ribosomes to a surface via biotin and streptavidin. The ribosomes are labeled with Cy5 at protein L11: (A) without streptavidin and (B) with streptavidin. (C) Polyphenylalanine assay for unmodified ribosomes (not biotinylated ribosomes) in solution and for surface-immobilized ribosomes. The background was measured in the absence of EF-G.

observation solution, incubated briefly at 37 °C, and then passed into the flow chamber.

RESULTS

SmFRET Experimental Design. The FRET pair consists of a ribosome containing protein L11 labeled with Cy5 (the FRET acceptor) at its unique native cysteine residue (Cys^{38}) and an EF-G variant (C113D/C265A/C397S/E231C), denoted E231C, labeled with Cy3 (FRET donor). The relative positions of the labeling sites on the ribosome, deduced from X-ray crystal structures docked into cryo-EM maps, are shown in Figure 1A.

We immobilize Cy5-containing ribosomes, which are also labeled with biotin, on glass coverslips coated with streptavidin (Figure 1B). Such attachment is almost completely dependent on the streptavidin−biotin interaction (Figure 2A,B and R. Stapulionis et al., manuscript in preparation), yielding ribosomes that retain almost full activity in poly(U)-dependent poly(Phe) synthesis. In the assay that is shown (Figure 2C), ribosomes are attached to streptavidin-coated polystyrene beads, which give more surface area per unit sample volume than a flat microscope coverslip. The bead surface is a good approximation for the glass coverslip, since the ribosomes are surface-attached by the same linkage in both cases and the remainder of the glass surface is passivated by Tween 20. Similar results are obtained with poly(Phe) synthesis directly measured on glass (not shown). In both the solution and surface poly(Phe) assays, there is an initial burst of synthesis and then a slower rate continuing

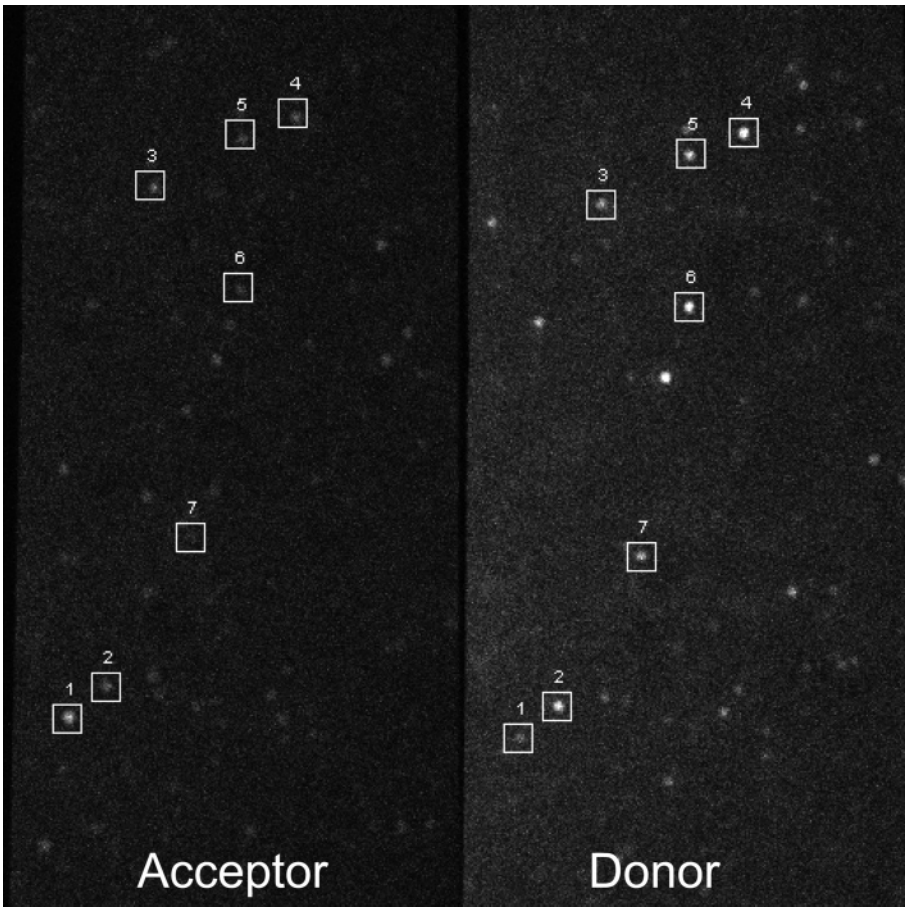

FIGURE 3: Split fluorescence image of a microscope slide with Cy3 emission (540−620 nm) on the right and Cy5 emission (640−740 nm) on the left. Numbered boxes identify examples of FRET pairs.

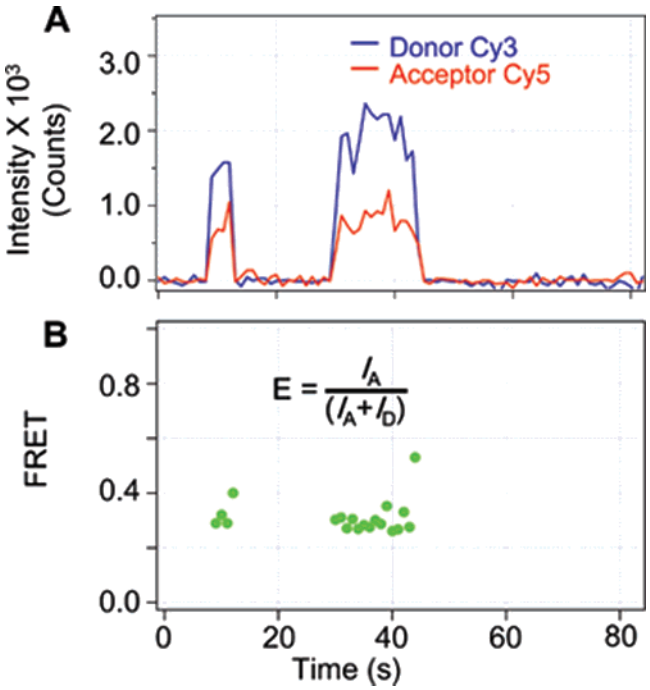

FIGURE 4: Representative fluorescence intensities and FRET efficiencies [$E = I_a/(I_a + I_d)$] as a function of time in a vacant ribosome.

for at least 30 min. These results closely parallel those reported previously (*26*).

In conducting smFRET experiments, we passed solutions containing Cy3-labeled EF-G past Cy5-labeled ribosomes immobilized on a microscope coverslip (see Materials and Methods). The sample is illuminated by glancing 514 nm laser light which produces evanescent wave fluorescence excitation of Cy3-EF-G when it binds to the immobilized ribosomes. Images of the fluorescence emission from both fluorophores are collected simultaneously at 1 s time intervals by splitting the emission into wavelength ranges of 550−620 nm for Cy3 and 640−740 nm for Cy5 and projecting the resulting images on an electron multiplying CCD camera (Figure 3 and the Supporting Information movie). The 1 s time interval for image collection and the illumination intensity are set as a tradeoff between rapid photobleaching of the fluorophores at higher laser intensities and a reduced signal-to-noise ratio at lower intensities. High DTT concentration, often used to delay photobleaching, compromised ribosome activities. This time resolution is sufficient to determine binding and dissociation rates of EF-G at the low factor concentrations used (see below) and fluctuations of intensity and FRET efficiency during poly-Phe synthesis.

In single-molecule TIRF microscopy, fluorescent labels diffusing in the solution, such as the free Cy3-labeled EF-G, are not detected by the camera because they diffuse into and out of the ∼100−200 nm deep evanescent wave much faster than the 1 s camera integration time. There is little direct excitation of Cy5-labeled ribosomes by 514 nm laser light. When EF-G binds to a ribosome, fluorescence emission is observed from Cy3 and, if the two fluorophores are sufficiently close, from Cy5 as well, via FRET. Correlated increases and decreases in fluorescence from both probes (Figure 4) thus indicate binding and dissociation of EF-G from the surface-bound ribosomes. As expected, when the surface did not contain tethered ribosomes, no pairs of recurring Cy3/Cy5 emission intensities were detected.

Donor and acceptor fluorescence intensities are quantified by fitting the paired Cy3 and Cy5 images with a 2D-Gaussian function, and the total intensity is calculated as $I = 2\pi A_0 \sigma_x \sigma_y$, where A_0 is the fitted peak intensity above background and σ_x and σ_y are the $1/e^2$ widths of the intensity peak, typically 1.5−2 pixels. During the bright intervals of EF-G binding, FRET efficiency is calculated as $E = I_a/(I_a + I_d)$, where I_a and I_d are the fluorescence intensities of the acceptor and donor, respectively. In Figure 4B, the FRET efficiency during the bright intervals is constant at ≅0.3.

Control experiments using unlabeled ribosomes and Cy3-labeled EF-G show that the microscope gives an optical leakage of ∼10% from emission of Cy3 into the Cy5 channel detector (Supporting Information, Figure S2). As a consequence, we limit consideration to those states having FRET efficiencies of >0.2. As the rotational mobility of the probes and relative sensitivities of the two detector channels were not determined, the FRET values observed are interpreted as providing estimates of relative rather than absolute distances in different states of the ribosome interacting with EF-G.

Vacant Ribosomes. We first assessed EF-G·GTP interaction with surface-immobilized ribosomes in the absence of mRNA and other components necessary for peptide synthesis. Binding of EF-G·GTP to vacant ribosomes in solution results in rapid GTP hydrolysis and dissociation of EF-G, either with or without GDP bound (*17*). With the surface-immobilized ribosomes, the donor and acceptor fluorescence traces repeatedly increased and decreased together (Figure 4A), resulting in a strong correlation between the two traces (correlation coefficient $r \cong +0.6$). This behavior indicates multiple turnovers of EF-G binding and dissociation from an individual ribosome. The FRET efficiency was ∼0.3, representing the peak value of a single Gaussian-shaped component in a population distribution of FRET efficiencies for EF-G molecules bound to vacant ribosomes (Figure 5A). This value is consistent with the ensemble FRET efficiency measured in a standard fluorometer (Figure 6). As explained in Materials and Methods, ensemble FRET values are calculated here from the decreases in donor fluorescence intensities.

When EF-G binds and produces donor and acceptor fluorescence, the two signals fluctuate with a standard deviation relative to the mean intensity [$\sigma_I/\langle I\rangle \cong 0.18$ (Figure 4A)], a value greater than would be expected purely from the statistics of photon counting at the camera gain in use (see Figure S3 of the Supporting Information and related text). These fluctuations are most likely due to photophysical events that cause the fluorophores to enter a transient dark state [i.e., "probe flickering" (*27*, *28*)]. Alternatively, the fluctuations could be attributed to rapid EF-G dissociation and/or rebinding events. However, this is unlikely, since the probability of such events occurring during individual 1 s camera frames is only 0.05, based on measured average durations of 2.9 and 5.6 s for bright intervals, and dark states between bright intervals, respectively [$(1 - e^{-1/2.9})(1 - e^{-1/5.6})$]. The duration of the dark state is as expected for the free concentration (10 nM) of EF-G utilized, given the known second-order rate constant for binding of EF-G to the ribosome (*15*).

Addition of the antibiotic fusidic acid (FA, 100 μM), which stabilizes binding of EF-G·GDP to the ribosome (*29*, *30*),

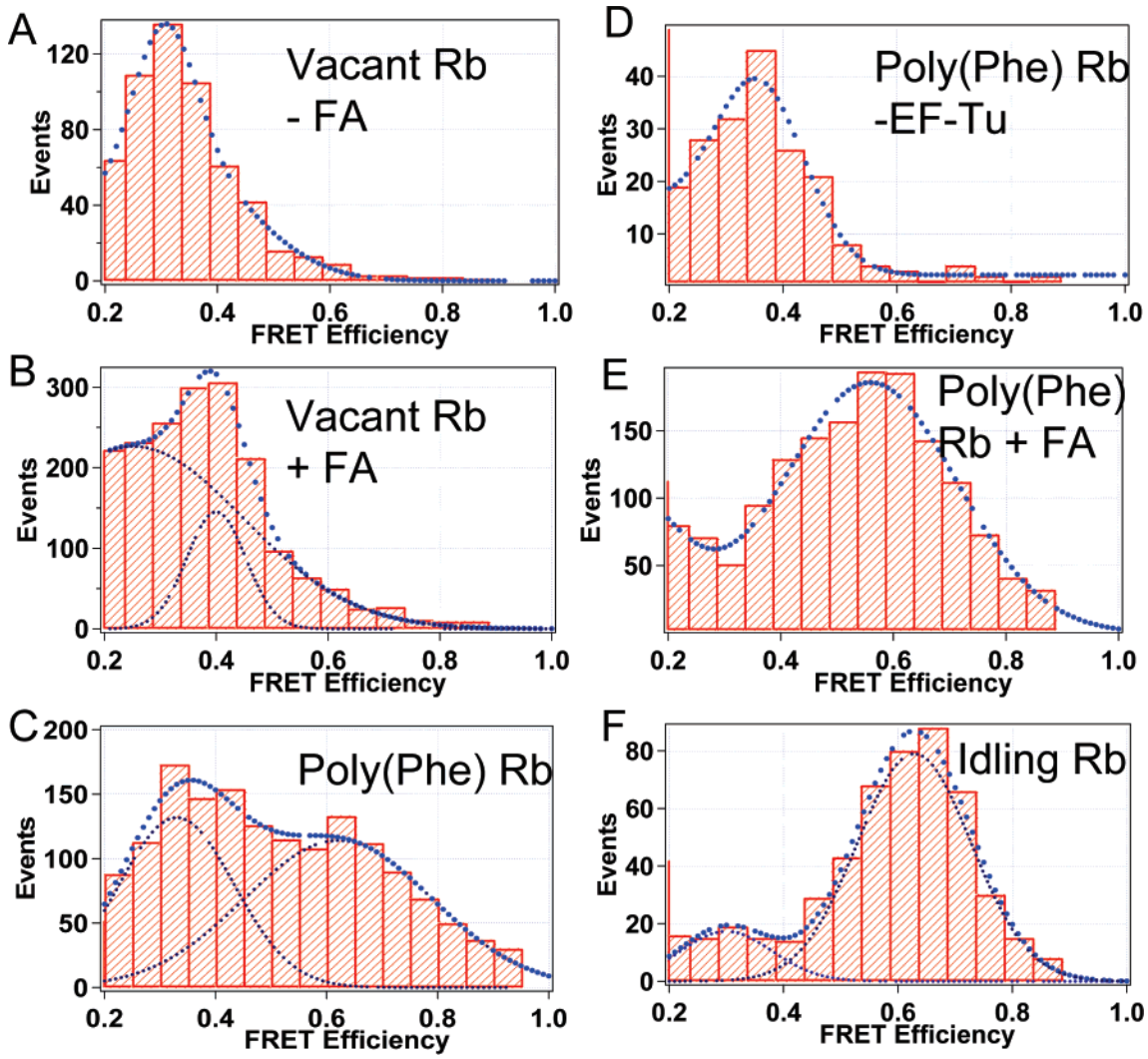

FIGURE 5: Population distributions of ribosome-bound EF-G intermediates: (A) vacant ribosome, (B) vacant ribosome in the presence of 100 μM fusidic acid, (C) ribosomes synthesizing poly(Phe), (D) poly(Phe) system in the absence of EF-Tu, (E) poly(Phe) system in the presence of 100 μM fusidic acid, and (F) idling poly(Phe) system ribosomes. FRET values of <0.2 are unreliable due to instrumental crosstalk between the donor and acceptor detection channels.

broadens the FRET efficiency distribution, which can be fitted with two Gaussian components, with peak values of 0.25 and 0.4 (Figure 5B). The higher overall FRET efficiency in the presence of fusidic acid agrees with the results of parallel measurements on ensemble samples of labeled ribosomes and EF-G·GTP, which show FRET efficiencies (E) of ≈0.26 in the absence of fusidic acid and ≈0.38 in the presence of 100 μM fusidic acid (Figure 6). These FRET efficiencies are somewhat higher than those obtained previously (E = 0.17 and 0.25) in the absence and presence of fusidic acid, respectively, using ribosomes labeled with fluorescein at the same site (Cys^{38} on L11) and EF-G labeled with coumarin at Cys^{216}. Coincidentally, this FRET pair has the same R_0 as Cy3-Cy5. The higher FRET efficiencies reported here are consistent with a structural model of EF-G bound to the ribosome, based on cryo-electron microscopy data [Figure 1 (*13*, *14*)], in which Cys^{38} of L11 is closer to EF-G Glu^{231} than to Gly^{216}.

Ribosomes Engaged in Polyphenylalanine Synthesis. Ribosomes were preincubated with poly(U), mRNA, and *N*-acetylphenylalanine-tRNA and then attached to the microscope slide surface. Other reaction components for poly(Phe) synthesis were delivered into the flow cell. In this case, FRET efficiencies were quite broadly distributed over the range of 0.2−0.8 (Figure 5C), with discernible peaks at E ≈ 0.3 and 0.6. This distribution indicates that the N-terminal domain of L11 can approach the G′ domain of EF-G considerably more closely in ribosomes engaged in polypeptide synthesis than on vacant ribosomes. The linkage of high FRET efficiency with actively translating ribosomes is confirmed by results obtained when EF-Tu is omitted, in which case the distribution of FRET efficiency values (Figure 5D) resembles that seen with vacant ribosomes. In the presence of fusidic acid, the E ≈ 0.6 state becomes dominant (Figure 5E), with a prolonged lifetime, often lasting for at least the full 200 s observation period. This behavior suggests that this antibiotic inhibits protein synthesis by binding to and stabilizing a normally transient intermediate that is formed during the elongation cycle. Implicit in this suggestion is the assumption that binding of fusidic acid to EF-G on the ribosome has no direct interaction with the covalently bound Cy3 that could modify its FRET efficiency with L11-Cy5, for example, by altering Cy3 mobility. This assumption is reasonable, since none of the proposed sites for binding of fusidic acid to EF-G are in the G′ domain (*31*).

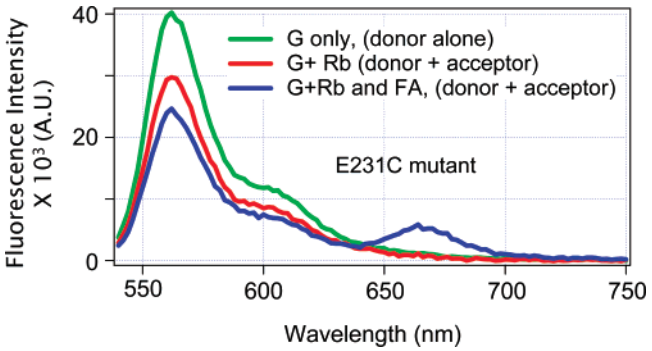

FIGURE 6: Fluorescence emission spectra of ensemble FRET between Cy3-EF-G-E231C (donor) and Cy5-L11-C38 ribosomes (acceptor). The excitation wavelength was 514 nm. The green trace is the fluorescence emission of the donor only (the solution contained labeled EF-G and unlabeled ribosomes). The red trace represents the data for the donor and acceptor (labeled EF-G and labeled ribosomes). The blue trace represents the data from the donor and acceptor in the presence of 100 μM fusidic acid. All of the traces are corrected for the background, including unlabeled ribosome light scattering and direct acceptor excitation. The solutions contained 0.36 μM ribosomes and 0.1 μM EF-G in TAM_{10} buffer in the presence of 1 mM GTP.

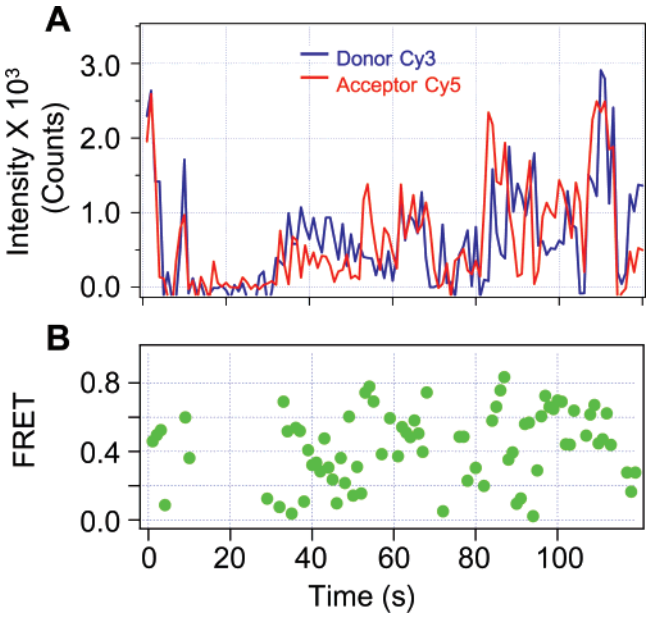

FIGURE 7: Representative fluorescence intensities and FRET efficiencies as a function of time when the ribosomes are synthesizing polyphenylalanine [poly(Phe) system].

The conditions of the single-molecule and ensemble poly(Phe) synthesis are different in several respects. In the single-molecule experiments, the EF-G concentration has been kept at a very low value (10 nM) to reduce background fluorescence from unbound molecules and nonspecific surface binding. The EF-Tu concentration is adjusted to 5-fold more than that of EF-G. On the other hand, in the ensemble poly(Phe) assay, the EF-G and EF-Tu concentrations are much higher (0.5 and 1 μM, respectively). Another important difference between our single-molecule experiments and the ensemble assay is the temperature (20 and 37 °C, respectively). These differences in experimental conditions cause poly(Phe) synthesis to proceed more slowly under the single-molecule conditions than in the traditional ensemble assay.

Ribosomes engaged in polyphenylalanine synthesis display time courses of fluorescence intensities and FRET efficiencies (Figure 7) that fluctuate considerably more than those found for vacant ribosomes (typically $\sigma_I/\langle I\rangle \cong 0.4$ as in Figure 7, vs ~0.18 in Figure 4). This result is consistent with the notion that active ribosomes are more flexible and dynamic than vacant ones. Since the EF-G concentrations and the surrounding medium are the same in both experiments, the probability of EF-G dissociating and rebinding during an individual camera integration time is very small, as in the case of the vacant ribosome. The rates of photophysical flickering and shot noise are also the same.

We observed periods with both positive and negative correlation coefficients between donor and acceptor fluorescence intensity signals, averaging +0.3 and −0.3, respectively, during binding of EF-G to ribosomes engaged in poly(Phe) synthesis. A negative correlation, which can be seen, for example, in the bright intervals of Figure 7, corresponds to the fluctuation of donor and acceptor fluorescence in opposite directions: an increase in donor fluorescence is accompanied by a decrease in acceptor fluorescence and vice versa. FRET efficiencies for time periods showing positive or negative correlation were, in both cases, quite broadly distributed, with the anticorrelated time periods showing a somewhat higher proportion of high-FRET ($E \approx 0.6$) periods. A significant fraction of the observed ribosomes (~20%) exhibited both correlated and anticorrelated fluctuations at different times, showing that such behaviors are not an indication of different ribosome populations. Rather, anticorrrelation most likely arises from conformational changes that alter the L11−EF-G distance on time scales comparable to our observation window.

Idling Ribosomes during Polyphenylalanine Synthesis. Some 2~3% of the observed ribosomes contained FRET pairs that were long-lived, lasting for the entire recording time of 200 s, even in the absence of fusidic acid. We denote these ribosomes as "idling", since elongation must be arrested when EF-G is bound continuously for several minutes or more. Idling ribosomes exhibited strongly anticorrelated donor and acceptor fluorescence intensities (Figure 8A, correlation coefficient ≅ 0.6) and had a FRET efficiency distribution resembling that seen for ribosomes in the poly(Phe) translation system in the presence of fusidic acid, with ~14% in the $E \approx 0.3$ state and ~86% in the $E \approx 0.6$ state (Figure 5F). These two states have average lifetimes of 0.65 and 3 s, respectively.

DISCUSSION

The results presented here, directed toward elucidating the motions of EF-G bound to the ribosome during the translocation step of the elongation cycle, are the first report of single-molecule fluorescence experiments during repetitive cycles of protein synthesis.

Ribosomes are thought to alternate between "locked" and "unlocked" conformations during elongation. Formation of a pretranslocation complex containing uncharged tRNA in the P-site and peptidyl tRNA in the A-site is thought to result in a conformationally labile or unlocked ribosome, predisposing the ribosome to major conformational changes upon EF-G·GTP binding and rapid GTP hydrolysis (*10*, *11*). Translocation is followed by a relocking step that may be rate-limiting for release of EF-G·GDP (*11*). When EF-Tu is omitted, the pretranslocation complex does not form, and

the presence of *N*-AcPhe-tRNA in the P-site would be expected to keep the ribosome in the locked conformation even when EF-G·GTP is bound and GTP is hydrolyzed.

Using smFRET, we demonstrate that both locked and unlocked ribosomes, as well as vacant ribosomes, can form a ribosome·EF-G·GDP complex having a FRET efficiency of ≈0.3. Only unlocked, translocating ribosomes can undergo the further conformational change to an *E* of ≈0.6 and even higher (Figure 5C), consistent with the greater flexibility of elongating ribosomes. The fraction of the ribosome·EF-G complex in the $E \approx 0.6$ state is enhanced in the presence of added fusidic acid, providing strong evidence that the antibiotic acts by preferentially binding to a preexisting ribosome·EF-G complex, rather than by inducing a new structure. Stabilization of the $E \approx 0.6$ state may inhibit the relocking step that appears to be necessary for rapid release of EF-G·GDP (*11*). Assuming that the attached fluorophores have relatively free rotation (i.e., $\kappa^2 = {}^2/_3$) and that instrumental corrections are small, the known R_0 value of ~50 Å for the Cy3-Cy5 FRET pair allows conversion of the FRET efficiencies of 0.3 and 0.6 into approximate distances between Cys^{38} in L11-NTD and Cys^{231} in the G′ domain of EF-G of 58 and 47 Å, respectively. The latter value is consistent with the distance (33 Å) between the β-carbon atoms of L11-NTD-Cys^{38} and G′-Cys^{231}, estimated from a cryo-EM-derived structure of the ribosome·EF-G·GDP·fusidic acid complex (*13*), taking into consideration the uncertainty introduced by the linkers and the sizes of the fluorophores themselves.

We also demonstrate a rare, long-lived, idling conformation in which the $E \approx 0.6$ state predominates over the $E \approx 0.3$ state (Figure 5F), opposite to the relationship between these states during normal translocation and elongation (Figure 5C). Ribosomes are known to pause or stall during polypeptide synthesis, due to rare codons (*32*), mRNA secondary structures (*33*, *34*), and pause-inducing nascent peptides inside the ribosome exit tunnel (*35*, *36*), possibly providing time for nascent peptide folding, frame shifting, skipping over secondary structure (*37*), or mRNA degradation (*38*, *39*). It is tempting to speculate that the small number of idling ribosomes we observe may correspond to an intrinsic paused or stalled state of the ribosome, although we cannot rule out the less interesting possibility that they are simply ribosomes that are damaged in some manner. Further work will be needed to resolve this issue.

Our results are most simply interpreted on the basis of Scheme 1, which posits two ribosome conformations, elongating and idling (it is unclear whether the two conformations are interconvertible and, if so, at what stages). During elongation, EF-G binding produces an initial complex with a FRET efficiency of ≈0.3, in which the relative orientation of the G′ domain of EF-G and L11-NTD probably resembles that found following GTP hydrolysis in our earlier ensemble FRET experiment examining the dynamics of the interaction of EF-G·GTP with vacant ribosomes (*15*). This complex then switches transiently to an $E \approx 0.6$ state as part of the translocation pathway. Fusidic acid freezes the ribosome in the $E \approx 0.6$ state and thus blocks elongation. Importantly, neither the transient $E \approx 0.6$ state of active ribosomes nor the idling conformation has been previously identified in ensemble structural (*10*, *13*, *14*, *40*) or kinetic

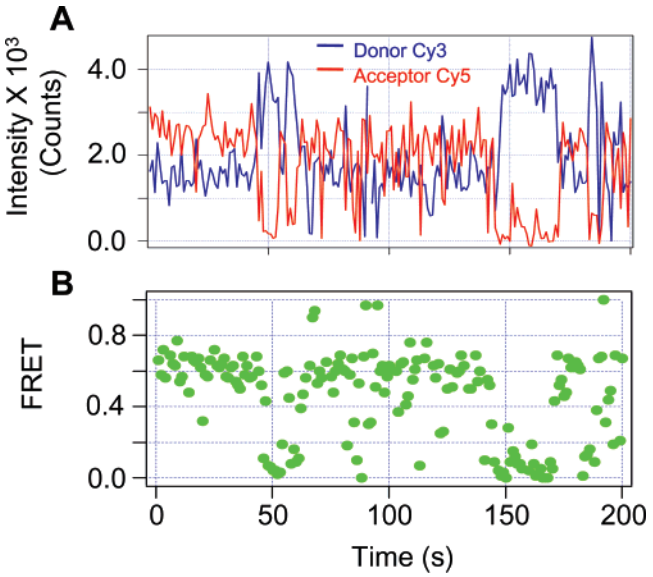

FIGURE 8: Representative fluorescence intensities and FRET efficiencies as a function of time for the idling state.

Scheme 1: Translocation Scheme Including Idling States and Inhibition by Fusidic Acid (FA)

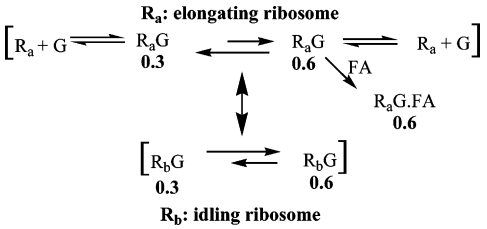

experiments (*11*, *15*), nor has the mechanism of action of fusidic acid been as clearly defined (*15*, *29*, *30*). These new findings thus provide a clear demonstration of the utility of single-molecule fluorescence microscopy in elucidating dynamical features of interaction of ribosome with protein factors and antibiotics.

SUPPORTING INFORMATION AVAILABLE

Results from an activity assay of Cy3-labeled EF-G (Figure S1), optical leakage of emission of Cy3 into the Cy5 detector channel (Figure S2), a trace of a single-molecule fluorescence showing signal variation due to pure photophysical fluctuations (Figure S3), and a sample movie of the surface-bound ribosomes in the poly(Phe) synthesis system collected at 1 s per frame. This material is available free of charge via the Internet at http://pubs.acs.org.

REFERENCES

1. Ban, N., Nissen, P., Hansen, J., Moore, P. B., and Steitz, T. A. (2000) The complete atomic structure of the large ribosomal subunit at 2.4 Å resolution, *Science 289*, 905−920.
2. Harms, J., Schluenzen, F., Zarivach, R., Bashan, A., Gat, S., Agmon, I., Bartels, H., Franceschi, F., and Yonath, A. (2001) High resolution structure of the large ribosomal subunit from a mesophilic eubacterium, *Cell 107*, 679−688.
3. Wimberly, B. T., Brodersen, D. E., Clemons, W. M., Jr., Morgan-Warren, R. J., Carter, A. P., Vonrhein, C., Hartsch, T., and Ramakrishnan, V. (2000) Structure of the 30S ribosomal subunit, *Nature 407*, 327−339.
4. Yusupov, M. M., Yusupova, G. Z., Baucom, A., Lieberman, K., Earnest, T. N., Cate, J. H. D., and Noller, H. F. (2001) Crystal structure of the ribosome at 5.5 Å resolution, *Science 292*, 883−896.

5. Schuwirth, B. S., Borovinskaya, M. A., Hau, C. W., Zhang, W., Vila-Sanjurjo, A., Holton, J. M., and Cate, J. H. (2005) Structures of the bacterial ribosome at 3.5 Å resolution, *Science 310*, 827−834.
6. Selmer, M., Dunham, C. M., Murphy, F. V., IV, Weixlbaumer, A., Petry, S., Kelley, A. C., Weir, J. R., and Ramakrishnan, V. (2006) Structure of the 70S ribosome complexed with mRNA and tRNA, *Science 313*, 1935−1942.
7. Korostelev, A., Trakhanov, S., Laurberg, M., and Noller, H. F. (2006) Crystal structure of a 70S ribosome-tRNA complex reveals functional interactions and rearrangements, *Cell 126*, 1065−1077.
8. Mitra, K., and Frank, J. (2006) Ribosome dynamics: Insights from atomic structure modeling into cryo-electron microscopy maps, *Annu. Rev. Biophys. Biomol. Struct. 35*, 299−317.
9. Nilsson, J., and Nissen, P. (2005) Elongation factors on the ribosome, *Curr. Opin. Struct. Biol. 15*, 349−354.
10. Valle, M., Zavialov, A., Sengupta, J., Rawat, U., Ehrenberg, M., and Frank, J. (2003) Locking and unlocking of ribosomal motions, *Cell 114*, 123−134.
11. Savelsbergh, A., Katunin, V. I., Mohr, D., Peske, F., Rodnina, M. V., and Wintermeyer, W. (2003) An elongation factor G-induced ribosome rearrangement precedes tRNA-mRNA translocation, *Mol. Cell 11*, 1517−1523.
12. Frank, J., and Agrawal, R. K. (2000) A ratchet-like inter-subunit reorganization of the ribosome during translocation, *Nature 406*, 318−322.
13. Datta, P. P., Sharma, M. R., Qi, L., Frank, J., and Agrawal, R. K. (2005) Interaction of the G′ domain of elongation factor G and the C-terminal domain of ribosomal protein L7/L12 during translocation as revealed by cryo-EM, *Mol. Cell 20*, 723−731.
14. Agrawal, R. K., Linde, J., Sengupta, J., Nierhaus, K. H., and Frank, J. (2001) Localization of L11 protein on the ribosome and elucidation of its involvement in EF-G-dependent translocation, *J. Mol. Biol. 311*, 777−787.
15. Seo, H. S., Abedin, S., Kamp, D., Wilson, D. N., Nierhaus, K. H., and Cooperman, B. S. (2006) EF-G-Dependent GTPase on the Ribosome. Conformational Change and Fusidic Acid Inhibition, *Biochemistry 45*, 2504−2514.
16. Pan, D., Kirillov, S. V., and Cooperman, B. S. (2007) Kinetically competent intermediates in the translocation step of protein synthesis, *Mol. Cell 25*, 519−529.
17. Wilden, B., Savelsbergh, A., Rodnina, M. V., and Wintermeyer, W. (2006) Role and timing of GTP binding and hydrolysis during EF-G-dependent tRNA translocation on the ribosome, *Proc. Natl. Acad. Sci. U.S.A. 103*, 13670−13675.
18. Blanchard, S. C., Kim, H. D., Gonzalez, R. L., Jr., Puglisi, J. D., and Chu, S. (2004) tRNA dynamics on the ribosome during translation, *Proc. Natl. Acad. Sci. U.S.A. 101*, 12893−12898.
19. Blanchard, S. C., Gonzalez, R. L., Kim, H. D., Chu, S., and Puglisi, J. D. (2004) tRNA selection and kinetic proofreading in translation, *Nat. Struct. Mol. Biol. 11*, 1008−1014.
20. Munro, J. B., Altman, R. B., O'Connor, N., and Blanchard, S. C. (2007) Identification of two distinct hybrid state intermediates on the ribosome, *Mol. Cell 25*, 505−517.
21. Wang, Y., Dempsey, G. T., Kudaravalli, R. D., Pan, D., Qin, H., Stapulionis, R., Knudsen, C. R., Cooperman, B. S., and Goldman, Y. E. (2006) Single molecule FRET of Ribosomes Immobilized on a Microscope Slide, *Biophys. J. 90*, 466a.
22. Stöffler, G., Cundliffe, E., Stöffler-Meilicke, M., and Dabbs, E. R. (1980) Mutants of *Escherichia coli* lacking ribosomal protein L11, *J. Biol. Chem. 255*, 10517−10522.
23. Robertson, J. M., and Wintermeyer, W. (1981) Effect of translocation on topology and conformation of anticodon and D loops of tRNAPhe, *J. Mol. Biol. 151*, 57−79.
24. Forkey, J. N., Quinlan, M. E., and Goldman, Y. E. (2005) Measurement of single macromolecule orientation by total internal reflection fluorescence polarization microscopy, *Biophys. J. 89*, 1261−1271.
25. Harada, Y., Sakurada, K., Aoki, T., Thomas, D. D., and Yanagida, T. (1990) Mechanochemical coupling in actomyosin energy transduction studied by *in vitro* movement assay, *J. Mol. Biol. 216*, 49−68.
26. Wagner, E. G., Jelenc, P. C., Ehrenberg, M., and Kurland, C. G. (1982) Rate of elongation of polyphenylalanine *in vitro*, *Eur. J. Biochem. 122*, 193−197.
27. Weiss, S. (1999) Fluorescence spectroscopy of single biomolecules, *Science 283*, 1676−1683.
28. Widengren, J., and Schwille, P. (2000) Characterization of photoinduced isomerization and back-isomerization of the cyanine dye Cy5 by fluorescence correlation spectroscopy, *J. Phys. Chem. A 104*, 6416−6428.
29. Bodley, J. W., Zieve, F. J., and Lin, L. (1970) Studies on translocation. IV. The hydrolysis of a single round of guanosine triphosphate in the presence of fusidic acid, *J. Biol. Chem. 245*, 5662−5667.
30. Bodley, J. W., Lin, L., Salas, M. L., and Tao, M. (1970) Studies on translocation V: Fusidic acid stabilization of a eukaryotic ribosome-translocation factor-GDP complex, *FEBS Lett. 11*, 153−156.
31. Martemyanov, K. A., Liljas, A., Yarunin, A. S., and Gudkov, A. T. (2001) Mutations in the G-domain of elongation factor G from *Thermus thermophilus* affect both its interaction with GTP and fusidic acid, *J. Biol. Chem. 276*, 28774−28778.
32. Varenne, S., Buc, J., Lloubes, R., and Lazdunski, C. (1984) Translation is a non-uniform process. Effect of tRNA availability on the rate of elongation of nascent polypeptide chains, *J. Mol. Biol. 180*, 549−576.
33. Tu, C., Tzeng, T. H., and Bruenn, J. A. (1992) Ribosomal movement impeded at a pseudoknot required for frameshifting, *Proc. Natl. Acad. Sci. U.S.A. 89*, 8636−8640.
34. Somogyi, P., Jenner, A. J., Brierley, I., and Inglis, S. C. (1993) Ribosomal pausing during translation of an RNA pseudoknot, *Mol. Cell. Biol. 13*, 6931−6940.
35. Nakatogawa, H., and Ito, K. (2002) The ribosomal exit tunnel functions as a discriminating gate, *Cell 108*, 629−636.
36. Murakami, A., Nakatogawa, H., and Ito, K. (2004) Translation arrest of SecM is essential for the basal and regulated expression of SecA, *Proc. Natl. Acad. Sci. U.S.A. 101*, 12330−12335.
37. Bucklin, D. J., Wills, N. M., Gesteland, R. F., and Atkins, J. F. (2005) P-Site pairing subtleties revealed by the effects of different tRNAs on programmed translational bypassing where anticodon re-pairing to mRNA is separated from dissociation, *J. Mol. Biol. 345*, 39−49.
38. Sunohara, T., Jojima, K., Yamamoto, Y., Inada, T., and Aiba, H. (2004) Nascent-peptide-mediated ribosome stalling at a stop codon induces mRNA cleavage resulting in nonstop mRNA that is recognized by tmRNA, *RNA 10*, 378−386.
39. Sunohara, T., Jojima, K., Tagami, H., Inada, T., and Aiba, H. (2004) Ribosome stalling during translation elongation induces cleavage of mRNA being translated in *Escherichia coli*, *J. Biol. Chem. 279*, 15368−15375.
40. Agrawal, R. K., Heagle, A. B., Penczek, P., Grassucci, R. A., and Frank, J. (1999) EF-G-dependent GTP hydrolysis induces translocation accompanied by large conformational changes in the 70S ribosome, *Nat. Struct. Biol. 6*, 643−647.

BI700657D